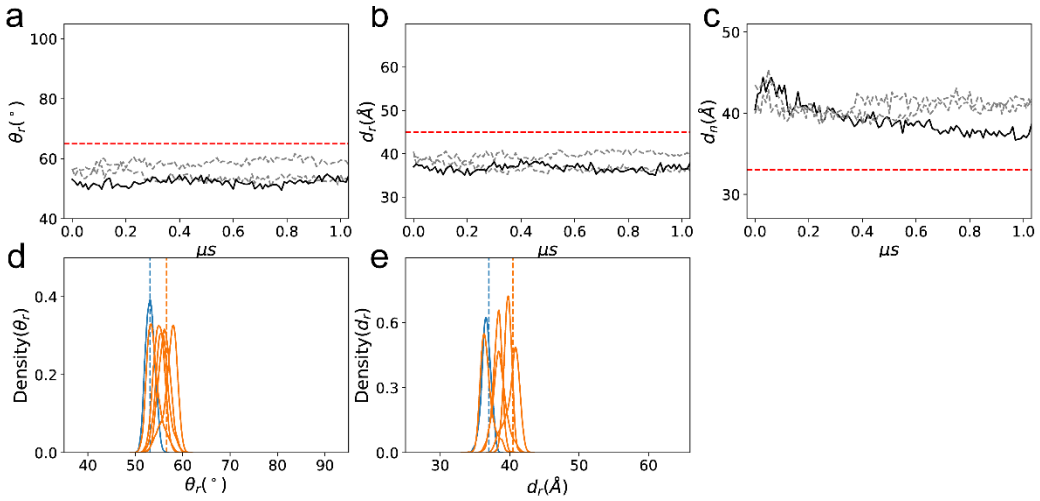

Figure S1. Illustration of the relative motions between the NTD and the downward RBD in the closed system. a-c, Evolution of the three metrics in the whole simulation. The downward RBD of chain C and its adjacent NTD of chain A in the closed system are picked from one repeat for evaluation. Chains with the selected NTD or RBD are illustrated in black solid lines, respectively, while the remaining chains are shown in grey dashed lines. The red dashed lines are shown as reference to capture the differences between simulation systems. d-e, Probability distributions of the angle (θr) and the distance (dr) as collected from the simulations to illustrate the movement of the downward RBDs of chain C (blue solid lines). The distributions of downward RBDs of chain A (orange solid lines) are taken as control. The blue dashed lines and the orange dashed lines indicate the corresponding values of the initial structures of the downward RBDs of chain C and chain A, respectively.

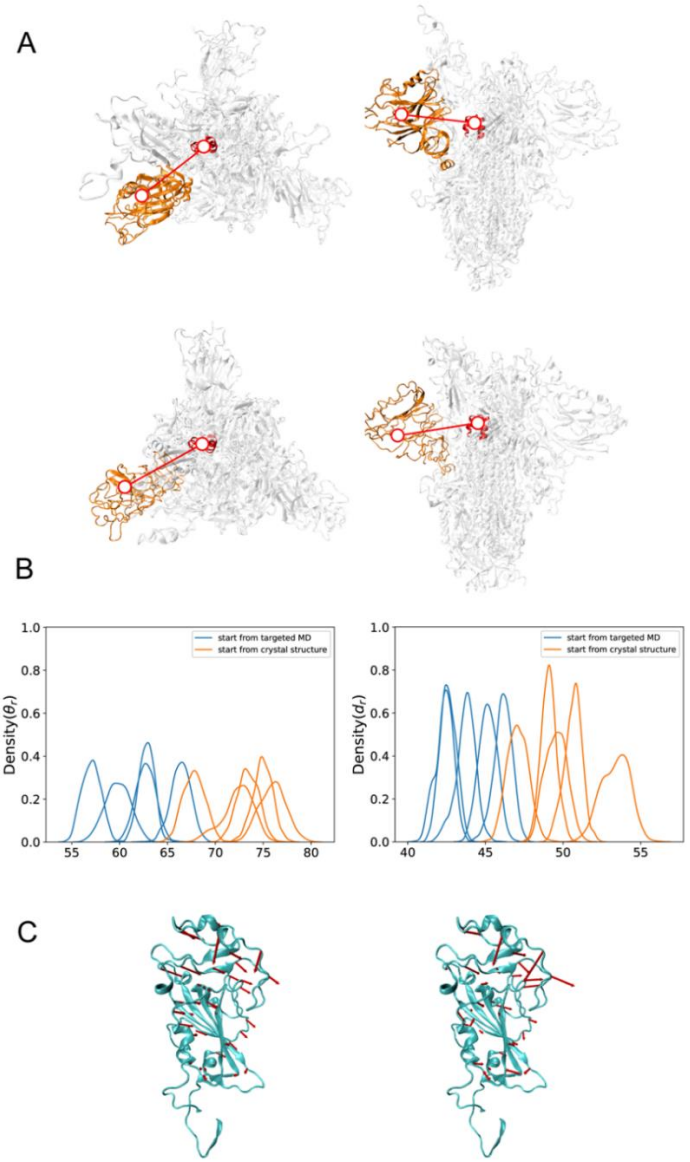

Figure S2. Illustration of conformational changes by aMD in the partially open system with the NTD forced out by the preceding tMD simulation. (A) Top view and side view of conformations before (top row) and after (bottom row) the simulation with tMD. The NTD of Chain C is highlighted in orange, and the central axis is highlighted in red. The blank line in the side view shows the distance between the center of the NTD and the central axis. (B) Distributions of RBD angle (θ_r) and RBD distance (d_r) of chain B. The last 200 ns trajectory in each repeat was used for evaluation. Trajectories starting from the NTD-forced-out state are colored blue, while those starting from the crystal structure are colored orange. (C) Analysis of slow motions of the RBD in the NTD-force-out simulations. Red arrows illustrate residue motions in the first principal component (left) and the first tIC (right) using snapshots from the first 200 ns.

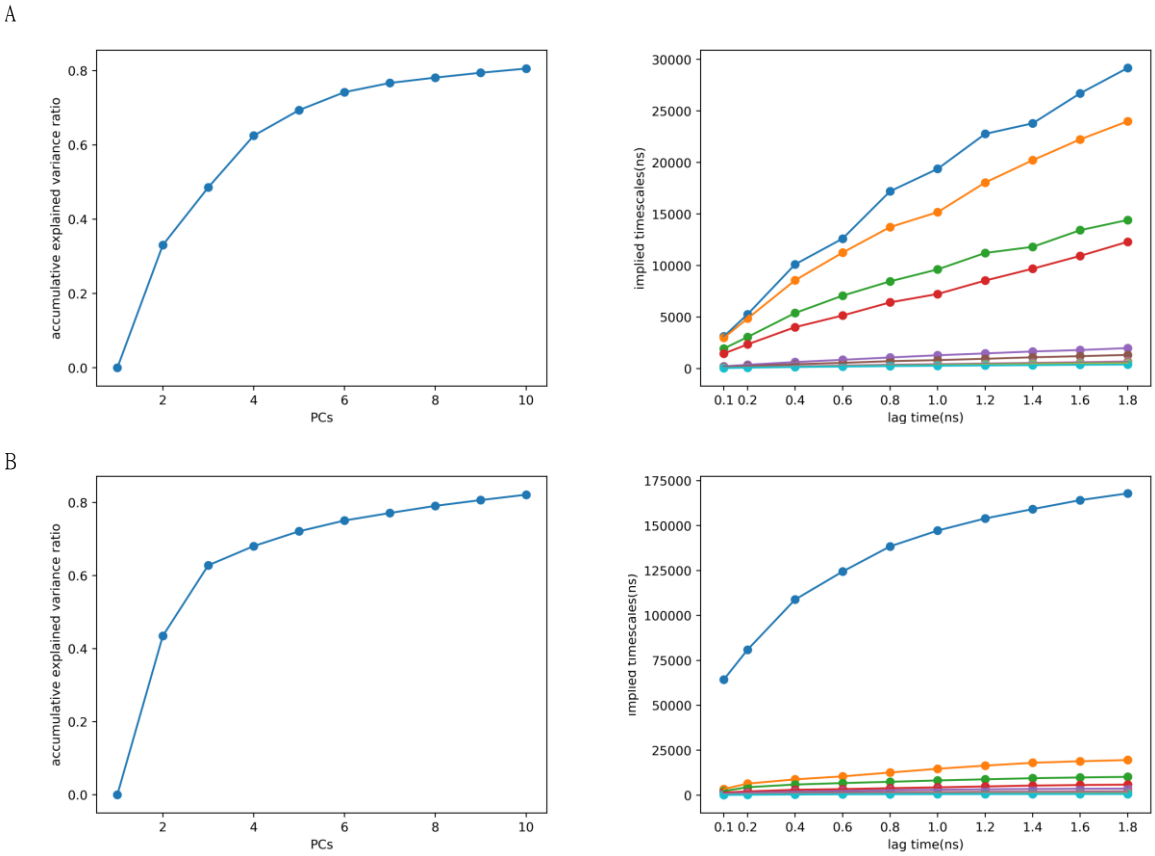

Figure S3. Illustration of parameter selection in the Markov State Model. (A) MSM in the partially open system to show the mode characterized by NTD wedging in and RBD being blocked. (B) MSM in the semi-open system to show the mode characterized by NTD moving out and RBD tilting downward. The left column shows accumulative variance ratios explained by top PCs, and the right column illustrates the first ten levels of timescales implied by the model with a chosen number of microstates of 100.

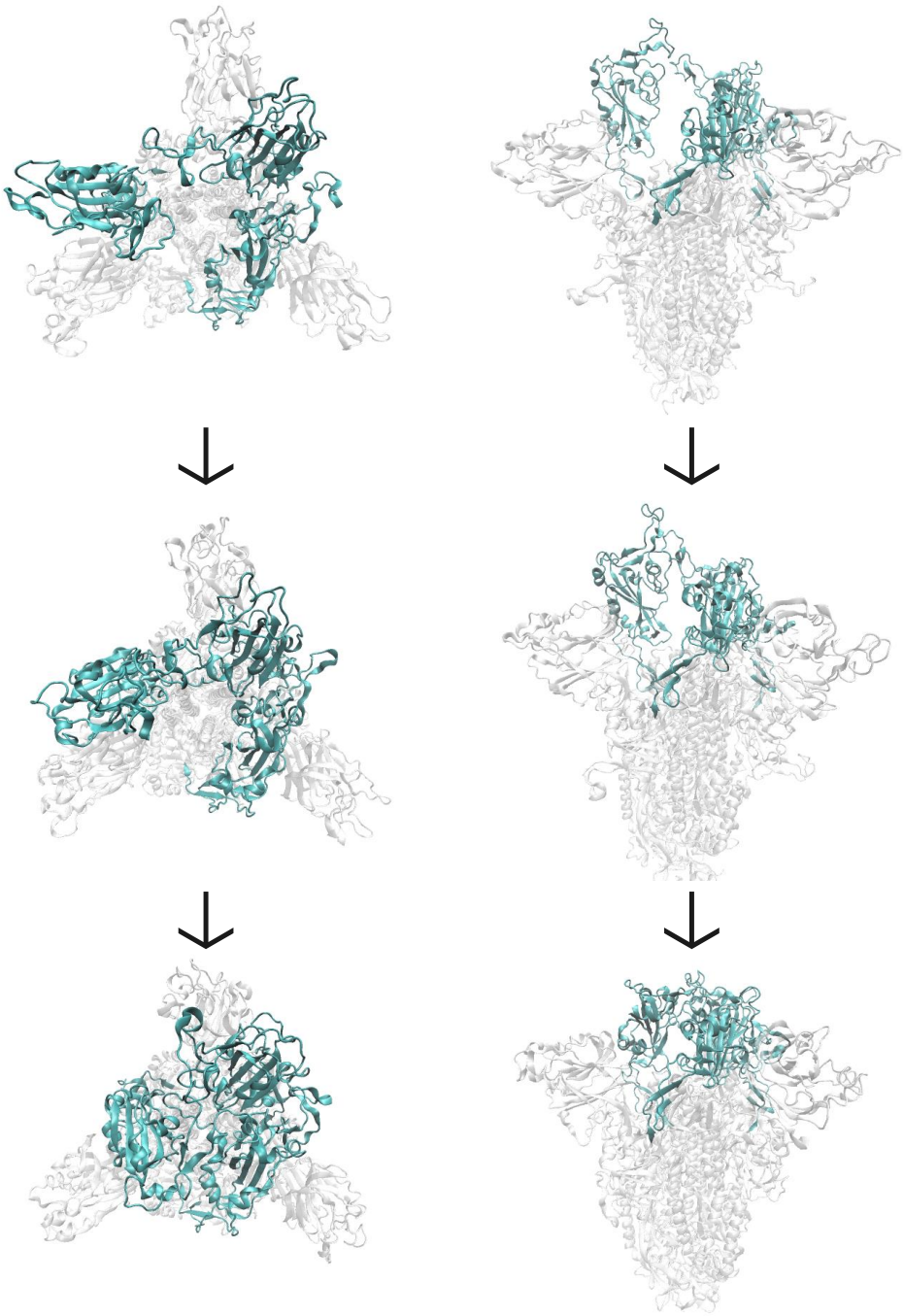

Figure S4. Interactions among RBDs in the semi-open system. The initial structure, a representative structure with two upward RBDs interacting with each other and a representative structure with all upward RBDs falling down to form close interactions are shown in the top, middle and bottom rows, respectively. The top view and side view are shown in the left and right columns, respectively.

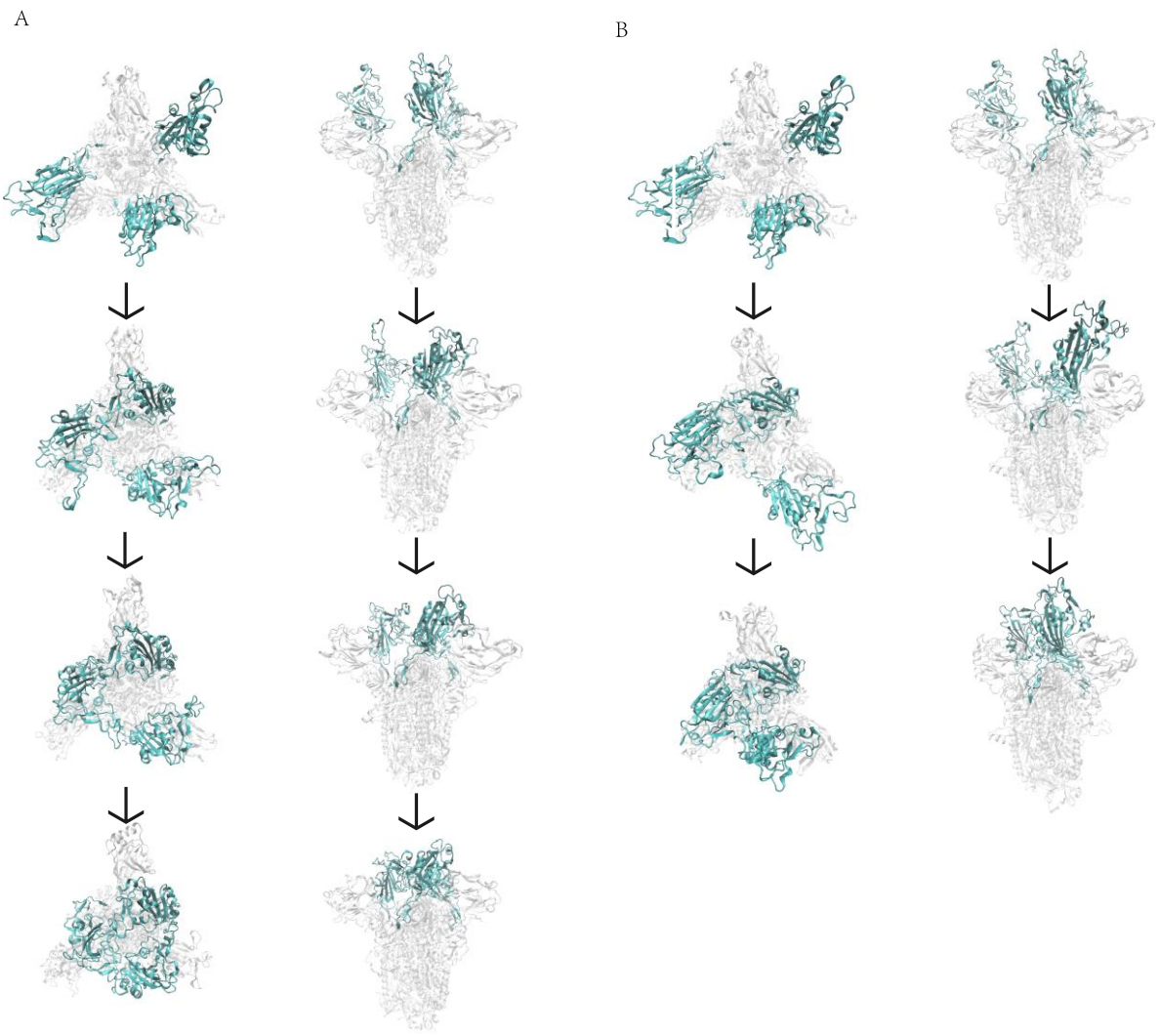

Figure S5. Interactions among RBDs in the open system. (A) A process with all three upward RBDs falling. Pairwise interactions between RBDs form gradually. (B) A process with two RBDs falling and one RBD remaining upright. Compared with (A), the RBD remaining upright formed interactions with only one RBD that tilted down.

Table S1. One-way ANOVA analysis of the relative motions of the NTD and the RBD in the simulation systems.

Simulation system	Mode	Category	df	F	P value
Partially open	NTD wedging in	Group	1	34.24188	<<0.01
		Error	8		
Semi-open	NTD wedging in	Group	1	168.197113	<<0.01
		Error	4		
Semi-open	NTD moving out	Group	1	0.601643	0.5191
		Error	2		
Open	NTD wedging in	Group	1	84.83	<<0.01
		Error	3		
Open	NTD moving out	Group	1	0.01	0.9275
		Error	3		

The average RBD angle of the last 200ns trajectory in each system was used for significance test.

Table S2. Key residue pairs lumped into different groups in the partially open system.

Lump	Macro 0	Macro 1	Macro 2	Macro 3	Macro 4	Macro 5
Green	R357-A163		R357-A163	R355-A163	R357-E132	R355-S162
			R357-N165	R357-C166	R357-N165	K356-Y160
			R357-C166	R357-T167	N394-N165	R357-V159
			R357-T167	R357-E169		R357-Y160
			R357-E169	N394-T167		R357-S161
				N394-F168		R357-S162
						R357-N164
						R357-C166
						S359-Y160
						N394-T167
Red			P521-P230	P521-Y200	H519-G232	H519-P230
				P521-P230	H519-I233	H519-I231
						H519-G232
						A520-P230
Yellow	P521-F168	P521-F168				A520-F168
						P521-F168
						P521-Y170
Purple	N360-T167			N360-F168	N360-T167	N360-E169
				N360-Y170	N360-E169	
Blue				R346-T160		

The first residue in each residue pair is the residue index of RBD in chain B and the second one is the residue index of NTD in chain C.

Table S3. Key residue pairs lumped into different groups in the semi-open system.

Lump	Macro 0	Macro 1	Macro 2	Macro 3
Green			T345-N164	
			T345-N165	
			R346-E132	
			R346-N165	
Red				N334-D198
				N334-Y200
				L335-P230
Brown				V367-Q115
				N370-T114
				N370-Q115
				N370-E132
				N370-N165
				N370-T167
				S371-Q115
				S373-E132
Purple		N334-T167		
		N334-F168		
Yellow		E340-K129		
		E340-C166		
		K356-E132		
		K356-N165		
Blue				E340-I233

The first residue in each residue pair is the residue index of RBD in chain B and the second one is the residue index of NTD in chain C.

Table S4. The top 20 chemical compounds with the highest binding affinities to the NTD in ZINC15 database.

Chemical compounds	Molecular Formula	Affinity (kcal/mol)
ZINC000261494659	C45H47NO18	-13.8
ZINC000261494656	C45H47NO18	-13.5
ZINC000261494657	C45H47NO18	-13.3
ZINC000169369935	C47H51NO15	-12.8
ZINC000169362007	C44H57NO17	-12.6
ZINC000261494658	C45H47NO18	-12.5
ZINC000085914855	C43H53NO14	-12.2
ZINC000003934128	C44H32N4O4	-12.2
ZINC000095627868	C43H59NO16	-12.2
ZINC000256109542	C35H54O11	-12.2
ZINC000256109534	C35H54O11	-12.1
ZINC000252286876	C47H75NO17	-12.0
ZINC000245190612	C47H75NO17	-11.9
ZINC000252286878	C47H75NO17	-11.9
ZINC000261494696	C24H34O5S	-11.8
ZINC000118915227	C24H34O5S	-11.7
ZINC000256109538	C35H54O11	-11.7
ZINC000245190613	C47H75NO17	-11.7
ZINC000169338351	C47H51NO15	-11.6
ZINC000169742991	C46H56N4O12	-11.6

Table S5. The detected compounds in the prescription for Han Shi Yu Fei Zheng.

Symptom	State of illness	Herb name	Detected compounds	Binding Affinity
Han Shi Yu Fei Zheng	Mild	Notopterygii Rhizoma Et Radix	chrysoeriol,7-rutinoside	-9.5
		Lepidii Semen Descurainiae Semen	evobioside	-9.9
			Helveticoside	-9.6
		Fortunes Bossfern Rhizome	Filicene	-9.7
		Eupatorium Fortunei Turcz	O-Acetyl-beta-amyrin	-9.6

Table. S6. The detected compounds in the prescription for Shi Re Yun Fei Zheng

Symptom	State of illness	Herb name	Detected compounds	Binding Affinity
Shi Re Yun Fei Zheng	Mild	Amomum Tsao-Ko Crevostet	quercetin,3-o-rutinoside	-9.8
		Anemarrhenae Rhizoma	Timosaponin B III	-10.5
			Tingenone	-10
			Smilagenin	-9.8
			Desglucolanatigonin II	-9.8
			Timosaponin A III	-9.8
			neogitogenin	-9.7
			Timosaponin A-III	-9.6
			xilingsaponin A	-9.5
			(-)-Caryophyllene oxide	-9.5
		Scutellariae Radix	5-o-caffeoylquinic acid	-9.8
		Radix Bupleuri	3'-O-Acetylsaikosaponin D_qt	-9.8
			Saikosaponin D	-9.7
			saikosaponin c	-9.5
			saikosaponin c_qt	-9.5
		Radix Paeoniae Rubra	Amyrin	-9.7
			Friedelin	-9.7
			Eugeniin	-9.7
			galloylpaeoniflorine	-9.7
		Forsythiae Fructus	C10230	-10.6
			Procyanidin	-9.7
			Forsythoside C	-9.5
		Artemisia Annua L.	artesunate	-9.9
			Friedelin	-9.7
		Isatidis Folium	Thladioside H1	-11.0
			6-(3-oxoindolin-2-ylidene)indolo[2,1-b]quinazolin-12-one	-9.9

Table S7. The detected compounds in the prescription for Shi Du Yu Fei Zheng

Symptom	State of illness	Herb name	Detected compounds	Binding Affinity
Shi Du Yu Fei Zheng	Moderate	Amygdalus Communis Vas	Licochalcone B	-9.5
		Pogostemon Cablin (Blanco) Benth.	Friedelin	-9.7
		Polygoni Cuspidati Rhizoma Et Radix	Chrysophanol-8-O-beta-D-(6'-O-galloyl)-glucopyranoside	-9.9
			Quercetin-3-rhamnoside-7-glucoside	-9.7
			(+)-Limacine	-9.6
		Verbenae Herb	beta-carotene	-9.6
			Scolymoside	-9.5
		Lepidii Semen	evobioside	-9.9
		Descurainiae Semen	Helveticoside	-9.6
		Citri Grandis Exocarpium	(2S)-7-[(2S,3R,4S,5S,6R)-4,5-dihydroxy-6-methylol-3-[(2S,3R,4R,5R,6S)-3,4,5-trihydroxy-6-methyl-tetrahydropyran-2-yl]oxy-tetrahydropyran-2-yl]oxy-5-hydroxy-2-(3-hydroxy-5-methoxy-phenyl)chroman-4-one	-9.5

Table S8. The detected compounds in the prescription for Han Shi Zu Fei Zheng

Symptom	State of illness	Herb name	Detected compounds	Binding Affinity
Han Shi Zu Fei Zheng	Moderate	Citrus Reticulata	(2S)-7-[(2S,3R,4S,5S,6R)-4,5-dihydroxy-6-methylol-3-[(2S,3R,4R,5R,6S)-3,4,5-trihydroxy-6-methyl-tetrahydropyran-2-yl]oxy-tetrahydropyran-2-yl]oxy-5-hydroxy-2-(3-hydroxy-5-methoxy-phenyl)chroman-4-one	-9.5
		Amomum Tsao-Ko Crevostet	quercetin,3-o-rutinoside	-9.8
		Notopterygii Rhizoma Et Radix	chrysoeriol,7-rutinoside	-9.5

Table S9. The detected compounds in the prescription for Yi Du Bi Fei Zheng

Symptom	State of illness	Herb name	Detected compounds	Binding Affinity
Yi Du Bi Fei Zheng	Severe	licorice	licorice-saponin F3	-10.1
			licorice-saponin K2	-10.1
			schaftoside	-10.1
			licorice-saponin F3_qt	-10.0
			Hispaglabridin B	-10.0
			beta-Glycyrrhetinic acid	-10.0
			18beta-glycyrrhetinic acid	-9.9
			licorice-saponin J2	-9.8
			glabrolide	-9.8
			Xambioona	-9.8
			Kanzonol Z	-9.7
			licorice-saponin H2	-9.6
			glycyrrhizin	-9.6
			isoglabrolide	-9.6
			Glycyram	-9.5
			licorice-saponin C2_qt	-9.5
			Araboglycyrrhizin	-9.5
		Amomum Tsao-Ko Crevostet	quercetin,3-o-rutinoside	-9.8
		Lepidii Semen	evobioside	-9.9
		Descurainiae Semen	Helveticoside	-9.6
		Radix Paeoniae Rubra	Amyrin	-9.7
			Friedelin	-9.7
			Eugeniin	-9.7
			galloylpaeoniflorine	-9.7

Table S10. The detected compounds in the prescription for Qi Ying Liang Fan Zheng

Symptom	State of illness	Herb name	Detected compounds	Binding Affinity
Qi Ying Liang Fan Zheng	Severe	Anemarrhenae Rhizoma	Timosaponin B III	-10.5
			Tingenone	-10.0
			Smilagenin	-9.8
			Desglucolanatigonin II	-9.8
			Timosaponin A III	-9.8
			neogitogenin	-9.7
			Timosaponin A-III	-9.6
			xilingsaponin A	-9.5
			(-)-Caryophyllene oxide	-9.5
		Radix Paeoniae Rubra	Amyrin	-9.7
			Friedelin	-9.7
			Eugeniin	-9.7
			galloylpaeoniflorine	-9.7
		Forsythiae Fructus	C10230	-10.6
			Procyanidin	-9.7
			Forsythoside C	-9.5
		Coptidis Rhizoma	Coptidis Rhizoma	-9.7
		Lepidii Semen	evobioside	-9.9
		Descurainiae Semen	Helveticoside	-9.6

Table S11. The detected compounds in the prescription for Nei Bi Wai Tuo Zheng

Symptom	State of illness	Herb name	Detected compounds	Binding Affinity
Nei Bi Wai Tuo Zheng	Very severe	Panax Ginseng C. A. Mey.	Araloside A	-9.9
			Campesteryl ferulate	-9.5
		Cornus Officinalis Sieb. Et Zucc.	Cornusiin A	-10.4
			Eugeniin	-10.1
			cornuside_qt	-9.7
			1,2,3-tri-O-galloyl-β-D-glucose	-9.6
			[(2R,3R,4S,5S,6R)-4,5-dihydroxy-2-(3,4,5-trihydroxybenzoyl)oxy-6-[(3,4,5-trihydroxybenzoyl)oxymethyl]oxan-3-yl] 3,4,5-trihydroxybenzoate	-9.5
			Cornusiin B	-9.5

Table S12. The detected compounds in the prescription for Fei Pi Qi Xu Zheng

Symptom	State of illness	Herb name	Detected compounds	Binding Affinity
Prescription for Fei Pi Qi Xu Zheng	convalescent	Citrus Reticulata	(2S)-7-[(2S,3R,4S,5S,6R)-4,5-dihydroxy-6-methylol-3-[(2S,3R,4R,5R,6S)-3,4,5-trihydroxy-6-methyl-tetrahydropyran-2-yl]oxy-tetrahydropyran-2-yl]oxy-5-hydroxy-2-(3-hydroxy-5-methoxy-phenyl)chroman-4-one	-9.5
		Codonopsis Radix	D-Friedoolean-14-en-3-one	-10.0
			Friedelin	-9.7
		licorice	licorice-saponin F3	-10.1
			licorice-saponin K2	-10.1
			schaftoside	-10.1
			licorice-saponin F3_qt	-10.0
			Hispaglabridin B	-10.0
			beta-Glycyrrhetinic acid	-10.0
			18beta-glycyrrhetinic acid	-9.9
			licorice-saponin J2	-9.8
			glabrolide	-9.8
			Xambioona	-9.8
			Kanzonol Z	-9.7
			licorice-saponin H2	-9.6
			glycyrrhizin	-9.6
			isoglabrolide	-9.6
			Glycyram	-9.5
			licorice-saponin C2_qt	-9.5
			Araboglycyrrhizin	-9.5

Table S13. The detected compounds in the prescription for Qi Yin Liang Xu Zheng.

Symptom	State of illness	Herb name	Detected compounds	Binding Affinity
Qi Yin Liang Xu Zheng	convalescent	Adenophprae Ae Radix	Praeruptorin A	-10.0
		Panacis Quinquefolii Radix	20(R)-Ginsenoside-Rh1_qt	-10.0
			ginsenoside- Rh1	-9.6
			ginsenoside Ro	-9.5
			Ginsenoside-Ra1	-9.5
		Mori Follum	Kwangsine	-11.2
			Inophyllum E	-10.0
			Morindin	-9.8
			Oxysanguinarine	-9.7
			Amyrin	-9.7
			Friedelin	-9.7
			beta-carotene	-9.6
			Albanol	-9.6
			Kuwanon H	-9.6
			O-Acetyl-beta-amyrin	-9.6
			Campesteryl ferulate	-9.5
		Phragmitis Rhizoma	b-AMYRIN	-9.8
		Radix Salviae	Neoprzewaquinone a	-11.0

Table S14. The parameters of the four simulation systems.

System	Initial structure	Chain length	Protein size (Å)	Water box size (Å)	Number of atoms	Ensemble
Closed	6VXX	1,134	135.361 135.540 164.449	207.362 214.892 187.271	787,311	NVT
Partially open	6VYB	1,134	133.234 144.632 183.832	211.978 222.469 213.915	950,940	NVT
Semi-open	Homology modeling from 6NB6	1,128	141.957 148.504 179.747	225.717 212.062 211.753	959,968	NVT
Open	Homology modeling from 6NB7	1,128	125.889 131.749 155.418	224.834 229.366 215.778	1,059,477	NVT

Movie S1. The movie of a replica of 1 microsecond accelerated MD for the closed system. Although the NTD of chain A has a trend of moving away from the central axis, all RBDs are finally locked in the "downward" conformation.

Movie S2. The movie of a replica of 1 microsecond accelerated MD for the partially open system. The upward RBD of chain B tends to tilt down while the adjacent NTD of chain C moves toward the central axis to prevent this downward movement.

Movie S3. The movie of a replica of 1 microsecond accelerated MD for the semi-open system. The upward RBD of chain B tends to tilt down while the adjacent NTD of chain A moves toward the central axis to prevent this downward movement.

Movie S4. The movie of a replica of 1 microsecond accelerated MD for the open system. The upward RBD of chain C tends to tilt down while the adjacent NTD of chain B moves toward the central axis to prevent this downward movement.

Movie S5. The movie of a replica of 1 microsecond accelerated MD for the semi-open system. The upward RBD of chain B reorients to the downward orientation when the NTD of chain A swings away from the central axis and then moves back to form a stable structure.

Movie S6. The movie of a replica of 1 microsecond accelerated MD for the open system. The upward RBD of chain B reorients to the downward orientation when the NTD of chain A swings away from the central axis and then moves back to form a stable structure.